J Mater Sci (2010) 45:3575–3587
DOI 10.1007/s10853-010-4402-y

Transient liquid phase diffusion bonding of 6061-13 vol.% SiCp composite using Cu powder interlayer: mechanism and interface characterization

Joydeep Maity · Tapan Kumar Pal · Rabindranath Maiti

Received: 5 November 2009 / Accepted: 8 March 2010 / Published online: 23 March 2010

Abstract Transient liquid phase diffusion bonding of an extruded 6061-13 vol.% SiCp composite at 560 °C, 0.2 MPa, using a 50-μm thick copper powder interlayer with 20 min, 1 h, 2 h, 3 h, and 6 h hold times has been investigated. The isothermal solidification and homogenization of the bond region occurred with 3 and 6 h holding, respectively. During isothermal solidification, smaller SiC particles (size range: 11–13 μm) were pushed by the moving solid/liquid interface and segregated around the bond centerline, whereas bigger SiC particles (size range: 24–33 μm) were engulfed. During isothermal solidification, the bigger SiC particles locally hindered the solidification front movement causing grain refinement. The kinetics of isothermal solidification, representing the displacement of the solid/liquid interface (y, in μm) as a function of time (t, in s), followed a power-law relationship: $y = 35\ t^{0.22}$. According to this kinetic equation, the effective diffusivity of copper in composite system was found to be about 10^5 times higher than the lattice diffusivity indicating the dominance of short circuit diffusion through the defect-rich particle/matrix interface. Ultrasonic investigation of the bond interface indicated that the signal attenuation was strongly correlated with the width of the segregated layer-a feature that decreased with the increasing bonding time. The completion of isothermal solidification was indicated by a sharp rise in the received signal amplitude with a negligible attenuation.

J. Maity (✉)
Department of Metallurgical and Materials Engineering, National Institute of Technology, Durgapur, Durgapur 713209, West Bengal, India
e-mail: joydeep_maity@yahoo.co.in

T. K. Pal
Welding Technology Center, Department of Metallurgical and Material Engineering, Jadavpur University, Kolkata 700032, West Bengal, India
e-mail: tkpal.ju@gmail.com

R. Maiti
Central Research Facility, Indian Institute of Technology, Kharagpur 721302, West Bengal, India
e-mail: maitirabin@yahoo.com

Introduction

The transient liquid phase (TLP) diffusion bonding process is an intriguing approach of joining which applies an interlayer between the pieces to be joined where the interdiffusion of the interlayer and the base material leads to the formation of a low-melting composition (eutectic) that melts, widens, shrinks, and solidifies at a fixed bonding temperature. The TLP diffusion bonding process was first introduced and patented by Paulonis et al. in the year 1972, in United States [1]. During that period the process was introduced for joining the heat resistant alloys, such as nickel-based superalloys [2]. Later on, along with the nickel-based superalloys (inconel, oxide dispersion strengthened (ODS) nickel alloy etc.), it has been also applied to other materials such as magnesium alloys, stainless steels, metal matrix composites, oxide and non-oxide ceramics, and dissimilar material joining (such as carbon/carbon composite to niobium alloy) [3–17].

The development of various metal matrix composites (MMCs) is regarded as a major advance in materials science and technology during the past few decades. The silicon carbide (SiC) reinforced aluminum-based metal matrix composites (AlMMCs) show better properties as compared to the monolithic aluminum alloys which make these composites useful for aerospace and transportation

industry applications [18, 19]. However, the difficulty encountered in their joining poses a major problem in the widespread industrial applications [20]. Mechanical fastening (bolting or riveting), fusion welding, and solid state diffusion bonding of such composites involve several difficulties [13, 14, 21–26] such as damage of reinforcement (for mechanical fastening); formation of brittle phase (Al_4C_3), cracking at the heat affected zone, and weld porosity (for fusion welding); and excessive plastic deformation under high applied pressure (for solid state diffusion bonding). The TLP diffusion bonding process has been reported as a promising technique by several investigators for joining the AlMMCs [12–17]. Extensive research work has been carried out on the mechanism and different stages of the TLP diffusion bonding process for pure metals or monolithic systems by Duvall et al. [2], MacDonald and Eagar [27], Tuah-Poku et al. [28], North et al. [29], and others [30, 31] which envisage the existence of four main stages namely, (I) dissolution of the interlayer, (II) homogenization of the liquid (widening of liquid to its maximum width), (III) isothermal solidification, and (IV) homogenization of the bond region at solid state. The duration of the first stage is only a few seconds, and the first two stages together take a few seconds or a few minutes, depending on the system. On the other hand, duration of the last two stages may extend to several hours. The process has advantages of a low bonding temperature, low bonding pressure, absence of a heat affected zone, disruption of the surface oxide film by the transient liquid phase, and a low probability of unfavorable reaction [2, 14, 28, 30]. In this joining process, the bonding temperature is kept slightly above the eutectic temperature of the interlayer-base material system and below the solidus temperature of the base material. The most widely used interlayer in TLP diffusion bonding of AlMMCs is the Cu since it involves a low bonding temperature (the eutectic temperature of the Al–Cu system is 548 °C) which is far enough below the solidus temperature of base material to prevent the melting or distortion. Out of the different stages of the TLP diffusion bonding process, isothermal solidification is the most important stage. If isothermal solidification is not completed, residual liquid may solidify as brittle phases impairing the joint strength [30]. In pure or monolithic systems, the kinetics of isothermal solidification has been extensively studied. The well-known kinetic equation representing the relationship between the solid/liquid interface displacement (y) with time (t) during isothermal solidification in pure or monolithic systems is given as:

$$y = k(4D_s t)^{1/2} \tag{1}$$

This expression was derived with an analytical treatment based on the classical theory of diffusion [27, 28, 31]. The other terms in this equation are the kinetic constant (k) and the diffusion coefficient of the solute in solid (D_s), since the isothermal solidification stage is mainly controlled by the diffusion in solid. However, a real system so often deviates from this analytical expression and the isothermal solidification kinetics may be represented [28] by a more generalized power law expression:

$$y = A\,t^{m} \tag{2}$$

where, 'm' is the system-dependent time exponent; and

$$A = k(4D_s)^{1/2}. \tag{3}$$

Although an extensive research has already been carried out on the mechanism and different stages of the TLP diffusion bonding process for the pure metals or monolithic systems [2–4, 6, 9, 11, 27–31], similar studies are not readily available for the AlMMCs. Also, in the investigations reported so far [7, 12–17] on the TLP diffusion bonding of AlMMCs, the bonding time has been kept low (maximum of 2 h) without any correlation with the completion of isothermal solidification or homogenization of the bond region. The major focus in these studies has been on the microstructure-property correlation in order to achieve adequate joint strength. The initial attempts by Bushby and Scott [12, 13] to join a SiC fiber reinforced AlMMC with 10-μm thick copper foil interlayer at 550 °C in air environment, resulted in a poor joint strength due to the oxidation of transient liquid. Klehn and Eagar [7] achieved better joint efficiency during the TLP diffusion bonding of 6061-15 vol.% Al_2O_3 in vacuum with Cu-foil and Ag-foil interlayers. Although the different stages of the TLP bonding process were not studied for composite system, the segregation of Al_2O_3 reinforcement at the bond interface was reported up to a maximum holding time of 2 h at 566 °C. In general, particle segregation at the bond region has been observed during the TLP diffusion bonding of AlMMCs containing alumina and silicon carbide, particle reinforced Cu, and when joining yttria-bearing oxide dispersion strengthened alloys [32]. The region of weakness produced by the particle segregation at the bond region has been found to promote preferential failure during tensile testing. A detailed study on particle segregation during the TLP diffusion bonding of 6061-20 vol.% Al_2O_3 composite using a Cu foil interlayer was carried out by Li et al. [32] based on the critical velocity concept of Stefanescu et al. [33] and Shangguan et al. [34] to explain the pushing and engulfment of insoluble particles by the advancing solid/liquid interface. It was found that the extremely slow rate of movement of the solid/liquid interface (much slower than the critical velocity) during the isothermal solidification stage of the TLP diffusion bonding process promotes particle segregation. In the 6061-Al_2O_3 system, particles less

than 30 μm size were found to be segregated at the joint region.

In order to further substantiate the progress of the TLP diffusion bonding process of AlMMCs, it is necessary to carry out a focused study on the mechanism of the different stages in correlation with the microstructural changes and the kinetics of isothermal solidification stage in the composite system. Furthermore, most ultrasonic nondestructive studies have been carried out on the fusion welded joints, and although echo amplitudes were found to be affected by the interface zone [35, 36], it is unclear whether similar behavior should be expected of TLP bonded AlMMCs. Therefore, the purpose of the present work is to study the microstructural variation at the joint region with regard to the process mechanism and kinetics during the TLP diffusion bonding of 6061-13 vol.% SiCp using a copper powder interlayer in an argon environment, and to investigate the effects of this process on ultrasonic attenuation through this joint.

Experimental procedure

Material, specimen preparation, and TLP diffusion bonding

The as-received material for the TLP diffusion bonding was an extruded rod of AlMMC consisting of 6061 matrix alloy (1.0 wt% Mg, 0.6 wt% Si, 0.3 wt% Cu, 0.2 wt% Cr, 0.6 wt% Fe, and balance Al) and 13 vol.% (15 wt%) silicon carbide (SiC) particulate reinforcement. The material was supplied by Regional Research Laboratory, Thiruvananthapuram, India, in the form of a cast billet with 23 μm average size of SiC particles (manufacturer's data). The cast billet was then extruded at National Metallurgical Laboratory, Jamshedpur, India, into a rod at 415 °C temperature with an extrusion ratio of 20:1. Thereafter, the size of SiC particles in the composite was measured to be 21 ± 5 μm (size range: 11–33 μm) by quantitative image analysis technique. During this measurement, the size was considered as an average of the major axis and the minor axis of an approximated elliptical particle in two-dimension. The extruded rod was machined to produce discs of 15 mm diameter and 10 mm in height. The faying surfaces of discs were polished at first with different grades of emery papers soaked in kerosene and liquid paraffin (1:1 proportion) up to 1000 grit, and finally with 1 μm diamond paste. Thereafter the surfaces were rinsed in acetone and dried by hot air blast. In order to maintain a copper powder interlayer of 50-μm thickness, initially a mass of 82 mg powder was taken. After applying copper powder between the discs, the assembly was pressed from both sides and set by an adhesive tape. During compaction (while pressing the assembly from both sides) some amount of powder was lost from the peripheral region of the cross section. Then the tape was locally dislodged at the joint region and the thickness of the powder interlayer was measured under optical microscope with graduated eye piece. The thickness of 50-μm was fixed on several trials. Thereafter the weight gain of the assembly was measured in a digital microbalance (PRECISA-205A-SCS, Switzerland) to determine the actual mass of the powder interlayer. Considering all specimens, the mass of copper powder interlayer (in terms of mean ± standard deviation) was found to be 75 ± 2 mg. The assembly was then inserted inside the diffusion bonding unit (programmable electric furnace), where the bonding was carried out at 560 °C under 0.2 MPa pressure in an argon environment. A thermocouple inserted into the drilled hole in one of each pair of discs was used to monitor the bonding temperature. The bonding temperature (560 °C) was kept above the eutectic temperature (548 °C) of Al–Cu system [37] and below the solidus temperature (582 °C) of 6061 matrix alloy [38]. The specimens were heated to the bonding temperature at a rate of 6 °C/min, held at that temperature for five different lengths of time (bonding time)—20 min, 1 h, 2 h, 3 h, and 6 h and cooled down to 540 °C at a rate of 5 °C/min inside the furnace. The specimens were subsequently taken out of the furnace and allowed to air-cool.

Optical metallography

The bonded cylindrical samples were sectioned perpendicular to the bonding plane. The section was polished at first with different grades of emery papers soaked in kerosene and liquid paraffin (1:1 proportion) up to 1000 grit, and finally with 1 μm diamond paste. Thereafter these were etched with Keller's reagent. Both the qualitative and quantitative study of the microstructure around the bond interface was carried out using an optical microscope with digital photomicrography & image analysis facility (ZEISS, Imager.A1m; Dewinter, MICROCAM 5.01). The interface width, grain size, and SiC particle size were measured. Due to mass flow toward the periphery under the applied pressure, the interface width was not uniform across the diameter of the discs. Therefore, the interface width was measured at the 'periphery' and at the 'central region' of the bond interface. The bond centerline was 15 mm in length. The two edges of bond centerline, with each edge 3.5 mm in length, were considered as 'periphery'; while the remaining 8 mm in the middle was considered as the 'central region.' Fifty measurements were taken (for both at the periphery and at the central region) and the mean value with standard deviation has been reported as the interface width. The SiC particle size was measured on as-polished unetched specimens at the segregation zone and at the isothermally solidified zone by

quantitative image analysis technique. Ten image-frames were captured at each zone, sizes of the particles were measured and the average value has been reported. The size of an individual SiC particle was considered as an average of the major axis and the minor axis of an approximated ellipse.

Scanning electron microscopy and energy dispersive X-ray spectroscopy

As-polished sections were examined around the bond interface under a scanning electron microscope (JEOL, JSM-5800). Reasonable phase contrast was achieved in the back scattered electron image mode. Different phases were identified by the spot analysis using Energy Dispersive X-ray Spectroscopy (EDS) with built-in ZAF correction. Furthermore, the line scan for concentration variation of copper was carried out along a line lying perpendicular to the bond interface while keeping the bond centerline approximately at the middle.

Ultrasonic test

The bonded cylindrical samples were machined to a 10 mm diameter to eliminate defects at the periphery. Thereafter, the flat surfaces at two ends were ground with a belt grinder and polished with fine emery paper to remove oxides and surface irregularities. Subsequently, these specimens (18 mm in length × 10 mm in diameter) were used for through-transmission ultrasonic testing. The test was carried out using an ultrasonic instrument (Krautkramer Branson USL 38M, Hurth, Germany) with 10 MHz normal probes as the transmitter and receiver. During test, the longitudinal wave propagated perpendicular to the bond interface (along the length of the specimen). The effect of particle segregation on ultrasonic attenuation was studied.

Results and discussion

As-received composite

The optical microstructure of as-received extruded AlMMC, as shown in Fig. 1a, reveals very fine recrystallized grains (grain size of 19 μm) and SiC particles. The recrystallization temperature range of commercial aluminum alloys is 340–410 °C [39]. Therefore, during extrusion of the parent AlMMC at 415 °C, the recrystallization of matrix occurred. The back scattered electron image (Fig. 1b) and spot analysis also reveal that the iron impurity is present in the composite in the form of intermetallic phases of iron and aluminum, $FeAl_x$ (both $FeAl_3$ and Fe_2Al_5).

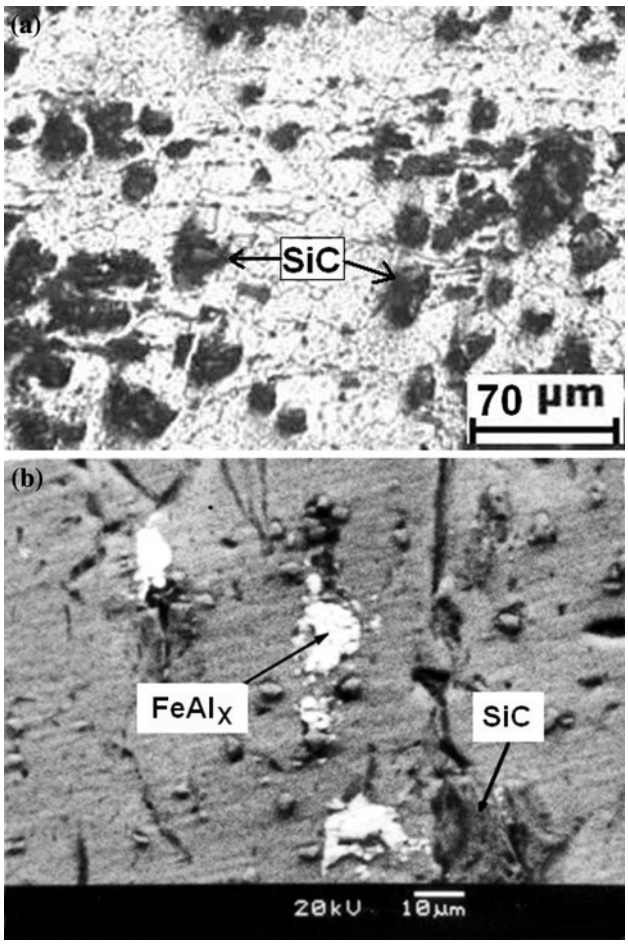

Fig. 1 Microstructure of as-received 6061-SiCp composite: **a** optical image; **b** back scattered electron image

Mechanism and microstructural evaluation

Optical microstructures of the TLP diffusion bonded polished and etched specimens representing the bond interface at the central region for different bonding conditions are shown in Fig. 2a–e. When etched with Keller's reagent the segregation zone (transient liquid mingled with the segregated SiC particles) appears dark. Adjacent to this, there exists an isothermally solidified zone containing the grains of isothermally solidified α. The remaining part consists of unaffected base material. The segregation zone (SZ), isothermally solidified zone (ISZ), and base material (BM) are labeled accordingly. Further finer details are depicted in the back scattered electron images of the bond interface (Fig. 3a–c). The isothermally solidified zone and the base material can be distinguished with more clarity through the presence of $CuAl_2$ precipitate in the isothermally solidified zone that appears as bright phase in back scattered electron image. The isothermally solidified zone is distinctly identified with the presence of isothermally solidified α grains (revealed in optical micrograph) along with the presence of

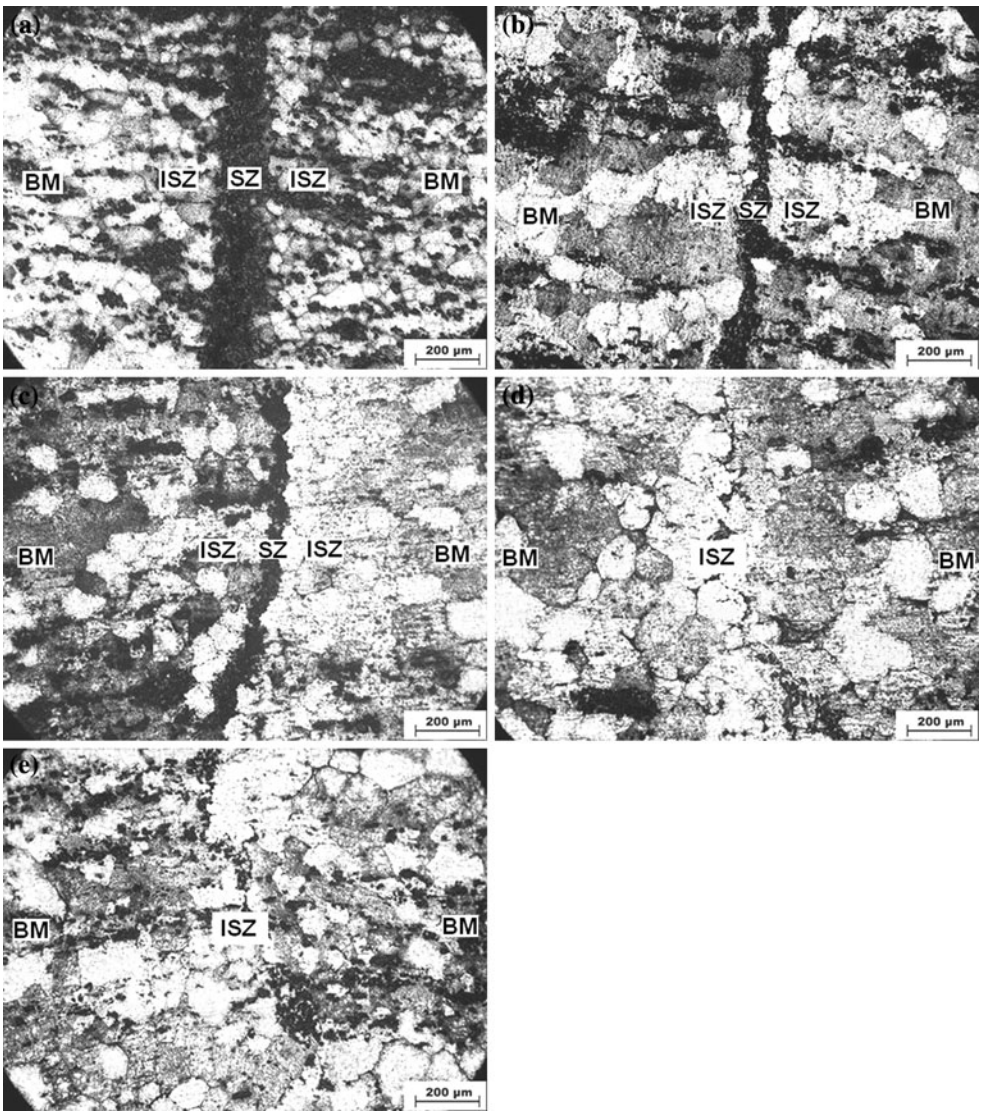

Fig. 2 Optical microstructures of bonded specimens representing the interface width at central region of the bond interface: **a** 20 min; **b** 1 h; **c** 2 h; **d** 3 h; and **e** 6 h. *SZ* Segregation zone, *ISZ* isothermally solidified zone, *BM* base material

$CuAl_2$ precipitates (revealed in back scattered electron image as bright phase). It is to be noted that the as-received AlMMC (unbonded) does not contain any $CuAl_2$ phase. In bonded composites, the $CuAl_2$ phase is precipitated out in the isothermally solidified zone during cooling from the bonding temperature as the solubility of Cu in primary α decreases with decreasing temperature following the solvus curve. Thus, when the microstructure is studied at room temperature, the presence of primary α grains along with $CuAl_2$ precipitates can be used to identify the isothermally solidified zone.

According to the study carried out by Natsume et al. [30] for joining pure aluminum by a 50 μm copper foil interlayer at 570 °C, the first two stages of the TLP diffusion bonding process are completed in 60 s. In the present study, heating from the eutectic temperature (548 °C) to the bonding temperature (560 °C) at a rate of 6 °C/min takes 2 min. Thus, it is most likely that the first two stages are completed during heating to the bonding temperature. Also the specimen with lowest bonding time (20 min) exhibits the presence of isothermally solidified zone adjacent to the bond interface (Figs. 2a, 3a). Therefore, the liquid widening process completes and isothermal solidification starts before 20 min of holding.

Progress of isothermal solidification

In this investigation, the presence of 13 vol.% SiC particle in 6061 aluminum matrix is expected to have a significant effect on the TLP diffusion bonding process as compared to monolithic systems. The degradation of SiC particles by chemical reaction with molten aluminum is feasible only

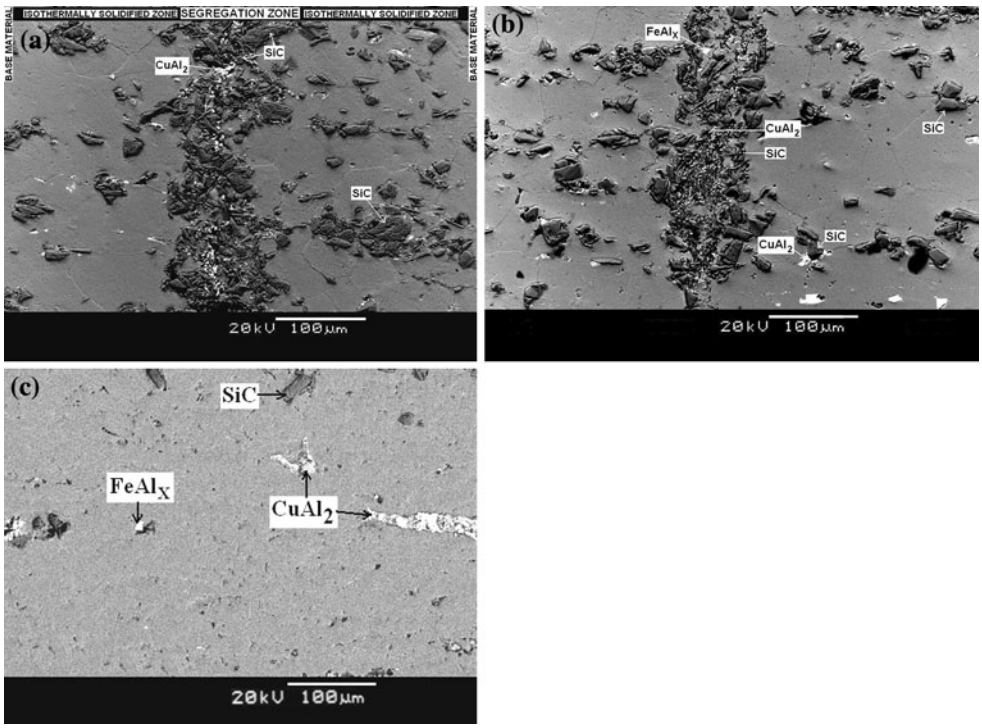

Fig. 3 Back scattered electron images of bonded specimens at central region of the bond interface: **a** 20 min; **b** 1 h; and **c** 6 h

above 727 °C [20]. Therefore, at the bonding temperature (560 °C) no chemical degradation of particle is possible. The major interaction would be the interaction between particles and the solidification front. Figures 2a–c and 3a and b reveal the segregation of SiC particles around the bond centerline with isothermally solidified zones on both sides. According to published literature [40] on the general solidification characteristic of SiC reinforced AlMMC, the primary α is very efficient at rejecting SiC, and pushing the particles ahead of the solid/liquid interface. In this regard, a critical velocity (V_c) of the solid/liquid interface has been reported, below which the SiC particles are pushed by the moving interface and above which they are engulfed [33, 34, 41]. In the TLP diffusion bonding process, during the widening of liquid, the solid/liquid interface moves away from the bond centerline; whereas, during isothermal solidification, the solid/liquid interface moves toward the bond centerline [28]. Since the first two stages of the TLP diffusion bonding (dissolution of the interlayer and widening of the liquid) are very fast, the velocity of the solid/liquid interface is also very high. As a result, during widening of the liquid, SiC particles are not pushed by the solid/liquid interface away from the bond centerline. The next stage, isothermal solidification, is comparatively slow due to the solid state diffusion controlling the process, typically taking several hours to complete. During isothermal solidification, due to the low velocity of the solid/liquid interface, most of the SiC particles of relatively smaller size are pushed by the moving solid/liquid interface and segregate around the bond centerline along with liquid phase; whereas the SiC particles of bigger size are engulfed. This is evident in Fig. 3a. Similar behavior of particle-pushing and segregation due to an extremely slow rate of movement of the solid/liquid interface during the isothermal solidification stage has been observed by Li et al. [32] in 6061-20 vol.% Al_2O_3 composite. The aggregate of the residual liquid and the segregated SiC particles may be called a 'Segregation Zone' and the width of this segregation zone may be termed the 'Interface Width'.

Therefore, in the present study, the bond region may be visualized as two zones, namely (i) the 'Segregation Zone' (just around the bond centerline), and (ii) the 'Isothermally Solidified Zone' (adjacent to the segregation zone). This is schematically shown in Fig. 4, and is indicated on the back scattered electron image in Fig. 3a. The measured interface width of the central region and at the periphery of the bond interface for different bonding conditions is presented in Table 1. At 20 min bonding time, the interface width at the central region is somewhat similar (slightly greater) to that at the periphery. However, with increasing bonding time, the interface width at the central region decreases continuously and always remains lower than that at the periphery. This phenomenon indicates that during the TLP diffusion bonding under pressure (0.2 MPa), the liquid–particle aggregate moves toward the periphery and flows out. Since the mass that flows toward the periphery is not simply liquid, but an aggregate of liquid and solid, a constriction to flow is likely to act at the periphery. Therefore,

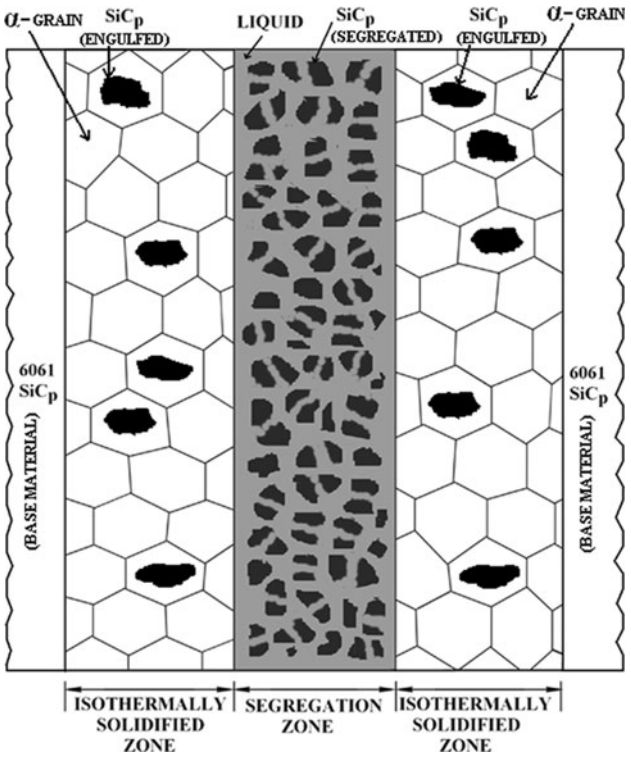

Fig. 4 Schematic representation of bond region during isothermal solidification

Table 1 Interface width at 'Central region' and 'Periphery'

Bonding time	Interface width (μm) (mean ± standard deviation)	
	At central region	At periphery
20 min	215 ± 14	204 ± 11
1 h	84 ± 7	186 ± 13
2 h	70 ± 5	126 ± 12
3 h	Negligible	131 ± 10
6 h	Negligible	127 ± 11

the interface width at the periphery depends on the accumulation of mass at periphery and its expulsion.

The flow of liquid toward the periphery under applied pressure has been investigated by Natsume et al. [30] while joining pure aluminum by a copper foil interlayer using the TLP diffusion bonding process. It has been established that the liquid expulsion under pressure and the diffusion-assisted isothermal solidification proceed simultaneously during the TLP diffusion bonding process. The mass flow under applied pressure eliminates some part of the liquid. This reduces the amount of liquid to be solidified isothermally, thereby shortening the duration of isothermal solidification [30]. Moreover, the mass flow toward periphery is likely to cause hindrance to the planar growth of solidification front. In monolithic system, the grain boundary diffusion is reported to be a reason of non-planar growth [42]. In composite system, the short circuit diffusion through the defect-rich regions of the particle/matrix interface is expected to play a dominant role in hindrance to the planar growth of solidification front. These factors result in a non-uniform interface width across the diameter, as observed in the present investigation.

Completion of isothermal solidification

The specimens subjected to 3 and 6 h bonding times exhibit negligible interface width in the central region with the least segregation of SiC particles, as shown in Figs. 2d, e and 3c. Furthermore, the bond interface is hardly discernible and the grain continuity exists across the interface indicating the completion of the isothermal solidification after a 3-h hold. Spot analysis of the matrix at the bond interface, after a 3-h hold, indicates the presence of 2 ± 0.3 wt% Cu (as per calculation of the mean and standard deviation values of the data obtained from ten spots). According to the Al–Cu phase diagram, at 560 °C, the maximum solubility of copper in primary α is 4.35 wt% [37]. Therefore, the copper content of 2 ± 0.3 wt% at the bond interface indicates the presence of primary α grains. This further confirms the completion of the isothermal solidification. It is important to note that, on completion of isothermal solidification, the central region is almost free of any particle segregation. However, the particle segregation still exists at the periphery (the interface width exists), as indicated in Table 1. The completion of isothermal solidification is supported by the presence of isothermally solidified primary α grains at the bond centerline. The simultaneous elimination of particle segregation in the central region is due to the flow of liquid–particle aggregate toward the periphery under the applied pressure. However, all the particles cannot flow outside the periphery. This causes segregation of particles at the periphery even on completion of isothermal solidification. The segregated particles at the bond interface have been reported as the regions of weakness [32]. Therefore, the elimination of particle segregation in the central region on completion of isothermal solidification is likely to produce a strong joint, once the region of particle segregation at the periphery is machined out.

Particle engulfment and nucleation of primary α grains

The microstructural analysis also reveals that during isothermal solidification, when the solid/liquid interface moves toward the bond centerline, some SiC particles are not pushed by the solid/liquid interface; rather they are engulfed (Figs. 3a, b, 5a, b). However, other SiC particles are pushed by the solid/liquid interface and agglomerated around the bond centerline forming a 'segregation zone' as

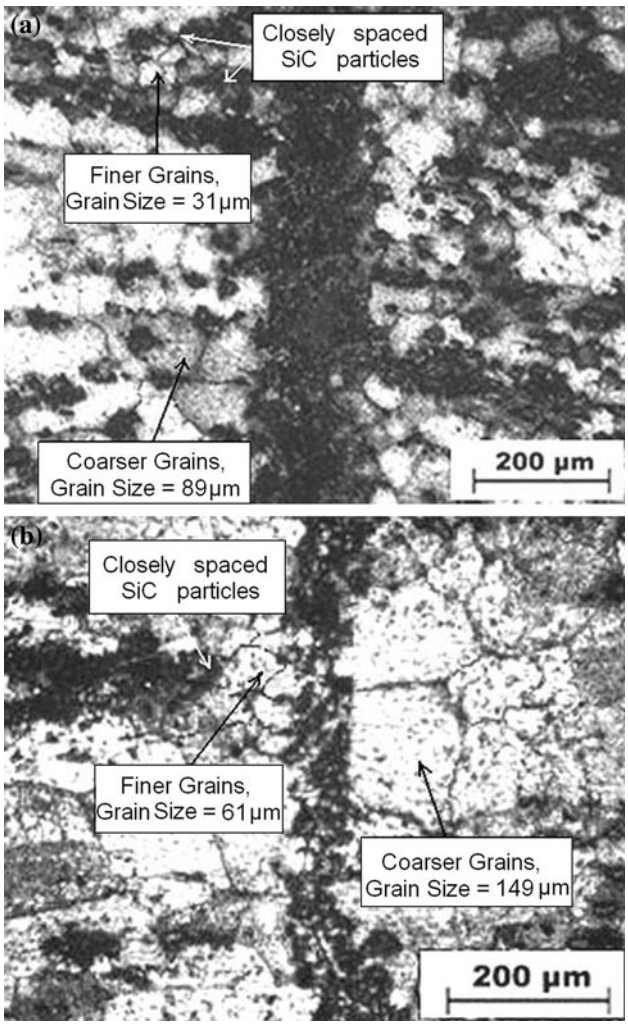

Fig. 5 Grain size variation in the isothermally solidified zone: **a** 20 min, central region; **b** 2 h, periphery

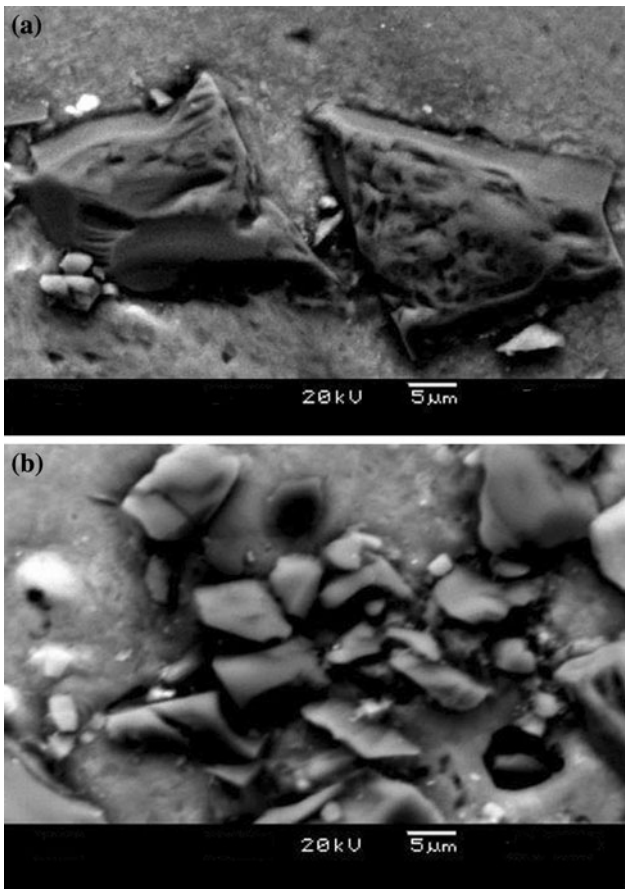

Fig. 6 Back scattered electron images representing SiC particle size: **a** isothermally solidified zone, 1 h; **b** segregation zone, 1 h

discussed earlier. The critical velocity determining the character of this zone depends on several factors including the particle size. It has been established that, the critical velocity (V_c) is inversely related to the particle size [33, 34, 41]. Therefore, bigger particles have a lower V_c and are likely to be engulfed, whereas smaller particles have a higher V_c and are likely to be pushed by the advancing solid/liquid interface. The size of the SiC particles in the 'segregation zone' (containing particles pushed by the solid/liquid interface during isothermal solidification) and at the isothermally solidified zone (containing engulfed particles) were measured. This is typically shown in Fig. 6. In general, considering all the bonding conditions, the particles in the isothermally solidified zone (engulfed particles) are found to be much bigger (size range: 24–33 μm) than the particles in the segregation zone (size range: 11–13 μm), as expected. This is also schematically presented in Fig. 4.

The distribution of engulfed SiC particles in the isothermally solidified zone is found to be non-uniform. Some part of the isothermally solidified zone is devoid of SiC particles, whereas some part is found to be particle-enriched. The particle-enriched regions so often contain closely spaced particles appearing as dark regions in optical image. The grain size of the primary α in the particle-enriched region is found to be much finer than the particle-devoid part. This is clearly evident in the optical microstructures as shown in Fig. 5a and b. The measured grain sizes are indicated for each microstructure. This observation indicates two possibilities: either the engulfed SiC particles act as nucleation sites for isothermal solidification, or these coarser particles cause local hindrance to the movement of the solidification front. During synthesis of ceramic particle reinforced aluminum metal matrix composites by casting route, it has been found that only the TiC particles (not the SiC or Al_2O_3 particles), due to their similarity in crystal structure with the aluminum alloy matrix (face centered cubic), act as heterogeneous sites for the nucleation of α-aluminum grains [43, 44]. On the other hand, Zhou and Xu [45] observed that during the solidification of 6061-20 vol.% SiC composite melt, the SiC particles of 25 μm size

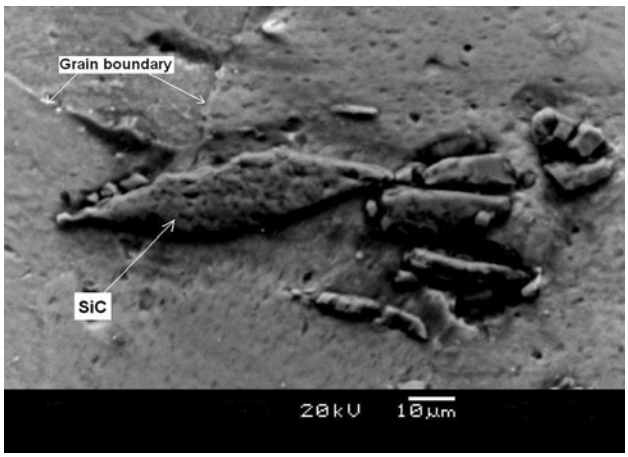

Fig. 7 Back scattered electron image of the isothermally solidified zone for 1-h holding representing the hindrance to the growth of solidification front by a particle enriched region

(coarser size similar to the size of SiC particles in the isothermally solidified zone of the present study) act as the local barrier to the growth of the solidification front. As a result, the solidification front splits to avoid the barrier that ultimately generates the finer grains around the particles. The similar phenomenon is found to occur in the present investigation as revealed in the back scattered electron image (Fig. 7) of the isothermally solidified zone in a polished and etched specimen. Accordingly, in the present investigation, grain refinement effect is observed in the particle enriched regions of the isothermally solidified zone.

Homogenization of the bond region and the presence of $CuAl_2$

The result of EDS line scan (Fig. 8) exhibits that the concentration of copper for 6-h holding is almost uniform

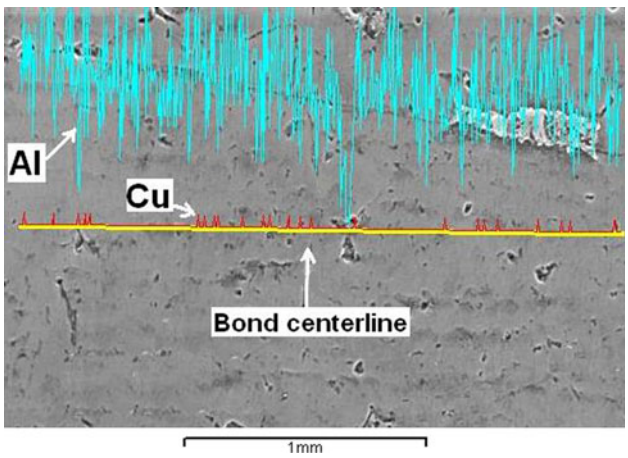

Fig. 8 Line scan result representing the concentration variation of Cu around the bond interface for 6 h holding

across the bond centerline indicating homogenization of the bond region. The $CuAl_2$ phase is found to be present in the segregation zone as well as in the isothermally solidified zone (Fig. 3a–c). At the bonding temperature, the segregation zone contains liquid intermixed with SiC particles. During cooling, while crossing the eutectic temperature (548 °C), the liquid solidifies through eutectic reaction: Liquid $\rightarrow \alpha + CuAl_2$. Again, while cooling below 548 °C to the room temperature, as the solubility of copper in primary α decreases with decreasing temperature, the $CuAl_2$ phase precipitates out of the eutectic α. Therefore, in the segregation zone, the $CuAl_2$ phase is present in the form of eutectic $CuAl_2$ and as $CuAl_2$ precipitates. Back scattered electron images (Fig. 3a, b) clearly reveal that during cooling, $CuAl_2$ preferentially nucleates on the SiC particles in the segregation zone. On the other hand, at the bonding temperature, the isothermally solidified zone contains isothermally solidified α grains and engulfed SiC particles. During cooling, as the solubility of Cu decreases, $CuAl_2$ precipitates out of the isothermally solidified α. Therefore, it is likely that, while studying microstructures at room temperature, the width of the total region containing $CuAl_2$ phase (considering the distance up to which $CuAl_2$ phase is present on both sides of the bond centerline) is an approximate estimate of the width of the total region affected by the TLP diffusion bonding process. The width of $CuAl_2$ containing region has been measured on SEM back scattered electron images for different bonding times. This is summarized in Table 2. With increasing bonding time, the width of the $CuAl_2$ containing region slowly increases due to the gradual diffusion of copper into the base material (6061-SiCp composite) beyond the region of maximum liquid widening (that solidifies isothermally) at the bonding temperature. During cooling, the precipitation of $CuAl_2$ is likely to occur in this narrow zone of the base material to which copper has diffused.

Process kinetics

Out of all the stages, the isothermal solidification is considered to be the most important stage in TLP diffusion

Table 2 Width of $CuAl_2$ containing region

Bonding time	Width of $CuAl_2$ containing region (μm)
20 min	536
1 h	542
2 h	547
3 h	553
6 h	558

bonding process. Completion of the isothermal solidification produces a single phase microstructure at the bonding temperature. If isothermal solidification is not completed, during cooling, the residual liquid solidifies eutectically that may generate brittle phases impairing bond strength [30]. Now, the displacement 'y' (expressed in μm) of the solid/liquid interface at a time of isothermal solidification 't' (expressed in s) is given as: $y = (W_{max} - W)/2$, where 'W' is the total width of the liquid phase (interface width) at the central region (considering the mean value) at an isothermal solidification time 't' and 'W_{max}' is the maximum width of the liquid phase. It is observed in Table 2 that the width of the $CuAl_2$ containing region does not vary significantly with bonding time. This indicates that the diffusion of solute (copper) into the base material beyond the region of maximum liquid widening is negligible, especially at lower holding time. Therefore, in the present study, the maximum width of liquid (W_{max}) may be approximated to 536 μm which is the width of the $CuAl_2$ containing region for 20 min of holding (the minimum holding time considered). Therefore, considering that the first two stages of the TLP diffusion bonding (interlayer dissolution and liquid widening) occur very fast and complete during heating to the bonding temperature, with $y = (536 - W)/2$ μm; four experimental data points viz. (1,200 s, 160.50 μm), (3,600 s, 226 μm), (7,200 s, 233 μm), and (10,800 s, 268 μm) are obtained for determining the kinetic expression of isothermal solidification. Using Microsoft Excel software, fitting these data points to the general form of governing equation of the isothermal solidification kinetics (power law relationship similar to Eq. 2), the relationship obtained is:

$$y = 35\, t^{0.22}. \tag{4}$$

This is presented in Fig. 9. A value (0.94) of the coefficient of determination (R^2) close to 1 and a small deviation of experimental data from this relationship (calculated as 4%) justify the acceptance of the developed equation. Now, with regard to Eq. 4, using an effective diffusion coefficient (D_e) for the composite system instead of lattice diffusion coefficient (D_s), Eq. 3 takes a form:

$$k(4D_e)^{1/2} = 35. \tag{5}$$

The system-dependent kinetic constant (k) follows the relationship [31]:

$$\frac{k(1 + \operatorname{erf} k)\pi^{1/2}}{\exp(-k^2)} = \frac{C_{\alpha L} - C_M}{C_{L\alpha} - C_{\alpha L}} \tag{6}$$

where 'C_M', the concentration of Copper (solute) in the base alloy, is 0.3 wt%. The other concentration terms ($C_{\alpha L}$, $C_{L\alpha}$) at the bonding temperature (560 °C) is determined from the Al–Cu phase diagram [37], as shown in Fig. 10. Accordingly, Eq. 6 becomes:

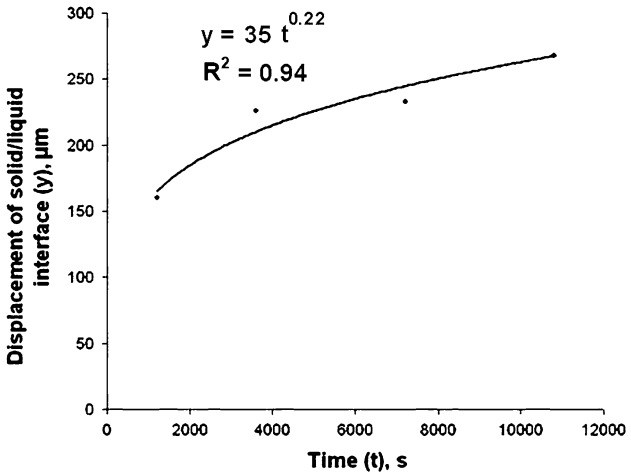

Fig. 9 Kinetics of isothermal solidification

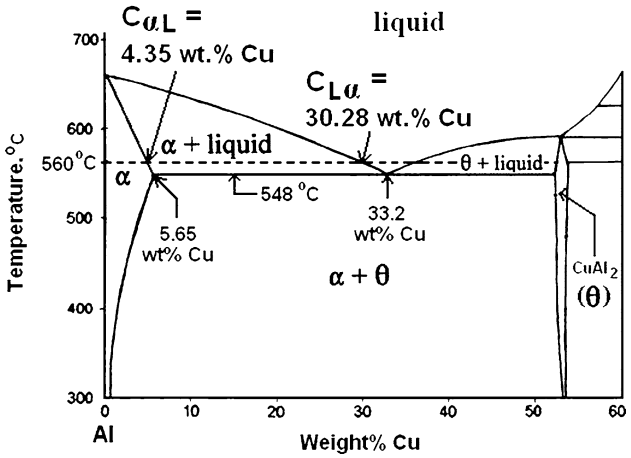

Fig. 10 Aluminum–copper phase diagram

$$\frac{k(1 + \operatorname{erf} k)\pi^{1/2}}{\exp(-k^2)} = 0.16. \tag{7}$$

Using Eq. 7 the value of 'k' is graphically calculated as 0.08 (Fig. 11). Putting this value in Eq. 5 the effective diffusion coefficient (D_e) in the composite is determined as 47,852 $\mu m^2\ s^{-1}$, i.e., $4.79 \times 10^{-8}\ m^2\ s^{-1}$. Now, knowing the values of the frequency factor and the activation energy for lattice diffusion of Cu in pure Al from the standard literature [30], D_s is calculated as $1.89 \times 10^{-13}\ m^2\ s^{-1}$. Therefore, the effective diffusion coefficient (D_e) in the composite system is about 10^5 times higher than the lattice diffusion coefficient (D_s) in the pure system. In the present study, the composite contains substantial amount (13 vol.%) of SiC particles. The presence of SiC particles in the metallic matrix leads to the formation of defect-rich interfacial region of high dislocation density, mainly due to the difference in the coefficient of thermal expansion between the metallic matrix and the SiC particles [46]. The coefficient of thermal

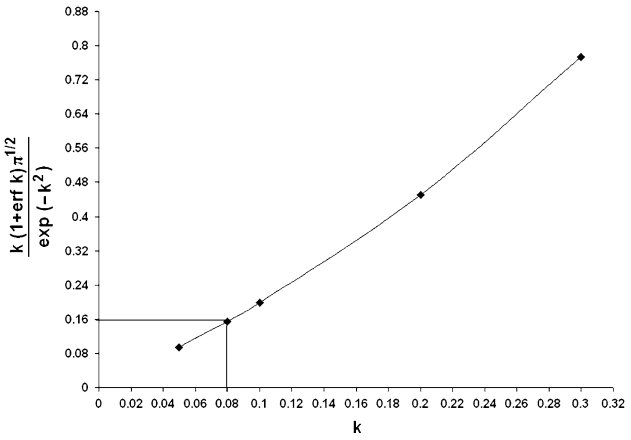

Fig. 11 Graphical determination of '*k*'

expansion of 6061 matrix alloy and SiC particle are 23.6×10^{-6} and 5.5×10^{-6} K^{-1}, respectively [38, 47]. Thus, it is likely that the particle/matrix interface of composite is associated with high dislocation density which provides short circuit paths for diffusion. It is reported that [48] the short circuit diffusivities are larger than the lattice diffusivities by a factor of 10^3 or more near the melting point or solidus temperature, as also observed in the present study. Therefore, at the bonding temperature of 560 °C (which is nearer to the solidus temperature, 582 °C, of 6061 alloy), the short circuit diffusion takes a significant role in the 6061-SiCp composite.

Segregation of $FeAl_x$

In the bonded composite, the particles or phases present in the segregation zone are mainly SiC and $CuAl_2$. However, at a few locations the intermetallic phases of iron impurity ($FeAl_x$) are also found to be present, as evident in Fig. 3b. The $FeAl_x$ is present in the parent composite. Thus, it is likely that during isothermal solidification, these $FeAl_x$ particles are pushed by the solid/liquid interface and thereby segregate around the bond centerline (at segregation zone) along with the SiC particles.

Ultrasonic characterization

The received signal height in terms of %FSH (Full Screen Height) has been measured form the oscilloscope display of the ultrasonic test which may be represented as the amplitude of the received signal. The received signal amplitude in correlation with the bonding time and the interface width (the width of particle segregation at the bond interface) at the central region for different bonding conditions is presented in Table 3. With increasing bonding time as the interface width decreases, the received signal height increases. For 10 MHz test frequency and with a sound

Table 3 Result of ultrasonic test

Bonding time	Interface width at central region (*W*) (μm)	Received signal amplitude (*A*) (%FSH)
20 min	215 ± 14	21
1 h	84 ± 7	35
2 h	70 ± 5	37
3 h	Negligible	97
6 h	Negligible	98

velocity of 6.32×10^3 m s^{-1} in aluminum [49], the wavelength of ultrasound comes out to be 632 μm. The particle size of the composite (21 ± 5 μm) is therefore less than 1/10th of the wavelength (63 μm). Under this condition, attenuation is usually absent [49]. Therefore, individual SiC particles do not cause attenuation of ultrasound. However, the increasing received signal height with bonding time indicates that the particle segregation at the bond interface causes attenuation of ultrasound. Once the diameter of the specimen is reduced to 10 mm from 15 mm for ultrasonic test, the interface width at the central region mainly represents the width of particle segregation. The width of particle segregation (interface width at the central region) is higher than the 1/10th of the wavelength (Table 3) and, therefore, is likely to cause significant scattering of ultrasonic wave. Since the particle segregation is aligned perpendicular to the ultrasonic wave, waves are scattered all around causing attenuation. The received signal amplitude as a function of bonding time is presented in Fig. 12. With increasing bonding time, the width of particle segregation at the central region decreases and accordingly attenuation also decreases due to the reduced scattering effect that is reflected as higher received signal height. The received signal height is very small (high attenuation) for the smallest bonding time (20 min). On completion of isothermal solidification (3 h holding or more), as the particle segregation at the central region is eliminated, the

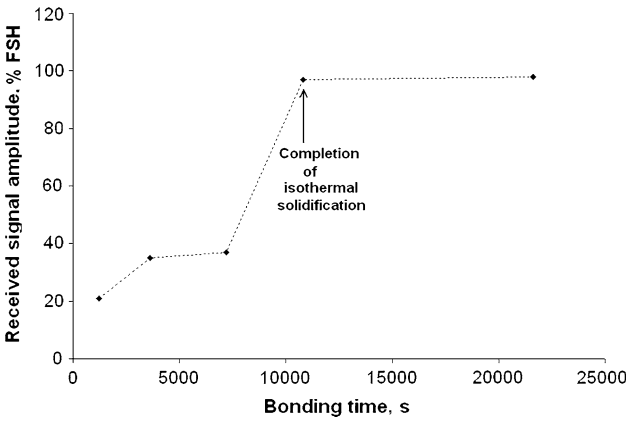

Fig. 12 Variation of the received signal amplitude with bonding time

received signal height suddenly increases and approaches close to the full screen height representing negligible attenuation. Therefore, this received signal amplitude versus bonding time plot (Fig. 12) may be useful to identify the completion of isothermal solidification stage. This identification is very much important since the completion of isothermal solidification ensures the least particle segregation and a better property of the TLP diffusion bonded joint.

Conclusion

(i) In the transient liquid phase diffusion bonding process of 6061-SiCp composite using a 50-μm thick copper powder interlayer at 560 °C under 0.2 MPa pressure, the isothermal solidification and homogenization of the bond region occur with 3- and 6-h hold times, respectively.

(ii) During isothermal solidification, the bigger SiC particles are engulfed; whereas, the smaller SiC particles are pushed by the advancing solid/liquid interface and segregate around the bond centerline along with the residual liquid. Simultaneously, under applied pressure the mass of residual liquid and segregated SiC particles moves toward the periphery and ultimately flows out with the increasing bonding time. During isothermal solidification, the bigger SiC particles locally hinder the growth of the solidification front, thereby generating finer grains.

(iii) The kinetics of isothermal solidification follows a power-law relationship: $y = 35\ t^{0.22}$. According to this relationship, the effective diffusivity of copper in the composite system was found to be about 10^5 times higher than the lattice diffusivity. This indicates the dominance of short circuit diffusion through the defect-rich particle/matrix interface.

(iv) The bond region consists of two zones, namely, (a) a 'segregation zone' (just around the bond centerline) and (b) an 'isothermally solidified zone' (adjacent to segregation zone). At the bonding temperature, the segregation zone mainly consists of residual liquid and SiC particles, and the isothermally solidified zone contains primary α and the engulfed SiC particles.

(v) On completion of isothermal solidification (3-h holding), the segregation of SiC particles remains only at the periphery; and the central region becomes segregation-free.

(vi) In the segregation zone, during cooling from the bonding temperature, the residual liquid undergoes eutectic solidification forming $CuAl_2$ and α. Upon further cooling, the $CuAl_2$ phase precipitates out of the eutectic α. In the isothermally solidified zone, $CuAl_2$ evolves only as a precipitate from the isothermally solidified α.

(vii) The segregated particles at the bond interface scatter ultrasonic wave causing attenuation. The extent of attenuation decreases as the width of the particle segregation decreases with increasing bonding time. The early stages of isothermal solidification are characterized by a high attenuation; whereas, a sharp increase in the received signal amplitude (low attenuation) indicates the completion of the isothermal solidification and the homogenization of the bond region.

Acknowledgement The authors are grateful to Mr. A. K. Shukla, Mr. D. Ghosh, Mr. A. Saha, Mr. S. Roy, and Mr. M. Maity of Central Mechanical Engineering Research Institute, Durgapur, India, for providing the ultrasonic testing facility and useful technical discussions.

References

1. Paulonis DF, Duvall DS, Owczarski WA (1972) United States Patent No. 3,678,570, July 1972
2. Duvall DS, Owczarski WA, Paulonis DF (1974) Weld J 53:203
3. Wikstrom NP, Ojo OA, Chaturvedi MC (2006) Mater Sci Eng A 417:299
4. Padron T, Khan TI, Kabir MJ (2004) Mater Sci Eng A 385:220
5. Li JL, Xiong JT, Zhang FS (2008) Mater Sci Eng A 483/484:698
6. Sun DQ, Liu WH, Gu XY (2004) Mater Sci Technol 20:1595
7. Klehn R, Eagar TW (1993) WRC Bull 385:1
8. Gale WF, Butts DA, Ruscio MD, Zhou T (2002) Metall Mater Trans A 33A:3205
9. Khan TI, Kabir MJ, Bulpett R (2004) Mater Sci Eng A 372:290
10. Khan TI, Roy BN (2004) J Mater Sci 39:741. doi:10.1023/B:JMSC.0000011546.44307.42
11. Egbewande AT, Chukwukaeme C, Ojo OA (2007) Mater Charact 59:1051
12. Bushby RS, Scott VD (1993) Mater Sci Technol 9:417
13. Bushby RS, Scott VD (1995) Mater Sci Technol 11:643
14. Shirzadi AA, Wallach ER (1997) Mater Sci Technol 13:135
15. Huang J, Dong Y, Wan Y, Zhao X, Zhang H (2007) J Mater Process Technol 190:312
16. Pal TK (2005) Mater Manuf Process 20:717
17. Yan J, Xu Z, Wu G, Yang S (2004) Scripta Mater 51:147
18. Huda D, El Baradie MA, Hashmi MSJ (1993) J Mater Process Technol 37:529
19. Lienert TJ, Baeslack WA, Ringnalda J, Fraser HL (1996) J Mater Sci 31:2149. doi:10.1007/BF00356639
20. Ellis MBD (1997) TWI J 6:69
21. Hall WI, Manrique F (1995) Scr Met 33:2037
22. Gittos MF, Threadgill PL (1991) Preliminary studies of joining particulate reinforced aluminium alloy metal matrix composites, metal matrix composites III: exploiting the investment, December 10–11, Inst. of Metals
23. Luhman TS, Williams RL, Das KB (1983) Development of joint and joining techniques for metal matrix composites, Fourth Quarterly Progress Report. Army Materials and Mechanics Research Center, pp 1–58
24. Devletian JH (1987) Weld J 66:33
25. Field DJ (1989) Aluminium alloys-contemporary research and applications. London Academic Press, UK

26. Urena A, Gomez De Salazar JM, Escalera MD (1995) Key Eng Mater 104–107:523
27. MacDonald WD, Eagar TW (1992) Annu Rev Mater Sci 22:23
28. Tuah-Poku I, Dollar M, Massalski TB (1988) Metall Trans A 19A:675
29. North TH, Ikeuchi K, Zhou Y, Kokawa H (1992) In: Cieslak MJ, Perepezko JH, Kang S, Glicksman ME (eds) Proceedings of the symposium on 'The metal science of joining'. The Minerals, Metals & Materials Society, Pennsylvania, pp 83–100
30. Natsume Y, Ohsasa K, Tayu Y, Momono T, Narita T (2003) ISIJ Int 43:1976
31. Zhou Y, Gale WF, North TH (1995) Int Mater Rev 40:181
32. Li Z, Zhou Y, North TH (1995) J Mater Sci 30:1075. doi: 10.1007/BF01178448
33. Stefanescu DM, Dhindaw BK, Kacar SA, Moitra A (1988) Metall Trans A 19A:2847
34. Shangguan D, Ahuja S, Stefanescu DM (1992) Metall Trans A 23A:669
35. Rogovsky AJ, Holmquist GR (1984) Mater Eval 42:318
36. Rogovsky AJ (1984) In: 3B Proc. Conf., Santa Cruz, CA, August 1983, Plenum Press, New York, pp 1063–1071
37. Anon (1992) Alloy phase diagrams, ASM handbook. ASM International, Ohio
38. Anon (1990) Properties and selection: non-ferrous alloys and special-purpose materials, metals handbook. ASM International, Ohio
39. Van Horn KR (1967) Aluminium—properties, physical metallurgy & phase diagrams. ASM International, Ohio
40. Gallerneault M, Kaya M, Smith RW, Dellamore GW (1991) In: Proc. conf. on extraction, refining and fabrication of light metals, Ottawa, Ontario, Canada, August 18–21, Pergamon Press Inc., New York, pp 69–81
41. Rohatgi PK, Asthana R, Das S (1986) Int Met Rev 31:115
42. Ikeuchi K, Zhou Y, Kokawa H, North TH (1992) Metall Trans 23A:2905
43. Karantzalis AE, Wyatt S, Kennedy AR (1997) Mater Sci Eng A 237:200
44. Kennedy AR, Wyatt SM (2000) Compos Sci Technol 60:307
45. Zhou W, Xu ZM (1997) J Mater Process Technol 63:358
46. Papazian JM (1988) Metall Trans A 19A:2945
47. Anon (1991) Ceramics and glasses, engineering materials handbook. ASM International, Ohio
48. Gjostein NA (1972) Papers presented at a seminar of the American Society for Metals, October 14–15, American Society for Metals, Metals Park, Ohio
49. Krautkramer J, Krautkramer H (1993) Ultrasonic testing of materials. Narosa Publishing House, New Delhi